# Experimental Investigation of Displacement Field around an Uplifting Anchor

Jinyuan Liu
*Ryerson University, Toronto, ON, Canada*
Mingliang Liu & Zhende Zhu
*Hohai University, Nanjing, China*

ABSTRACT
In this paper, a displacement field around a scaled semi-circular anchor during uplifting is obtained using digital image cross-correlation (DIC). DIC is a region-based image processing technique which can calculate the relative displacement field between two images. An optical test set-up is developed to capture the deformation during loading, which consists of a camera, a loading frame, and a PC. Two dry sand samples are used in the investigation: one is in loose condition and the other in dense. A series of images are taken from the camera while the anchor is being uplifted against the side-window of a Plexiglas mould. The displacement fields are calculated using DIC. The corresponding strain fields are deduced from the displacement fields. The results are consistent with published data. This model study improves the understanding of the failure and development of loading capacity of uplift anchor in cohesionless soil.

RÉSUMÉ
En ce document, un champ de déplacement autour d'une ancre semi-circulaire mesurée pendant élever est obtenu utilisant la corrélation croisée d'image numérique (DIC). DIC est une technique à traitement d'images région-basée qui peut calculer le champ relatif de déplacement entre deux images. Une installation d'essai optique est développée pour capturer la déformation pendant le chargement, qui se compose d'un appareil-photo, d'une armature de chargement, et d'un PC. Deux échantillons secs de sable sont employés dans la recherche : on est en état lâche et autre dans dense. Une série d'images est prise de l'appareil-photo tandis que l'ancre est élevée contre le side-window d'un moule de Plexiglass. Les champs de déplacement sont calculés utilisant DIC. Les champs de contrainte correspondants sont déduits des champs de déplacement. Les résultats sont compatibles aux données éditées. Cette étude modèle améliore l'arrangement de l'échec et du développement de la capacité de chargement d'ancre de soulèvement dans le sol cohesionless.

## 1 INTRODUCTION

Anchors, as an efficient and reliable anchorage system, has been widely used to resist uplift loads produced by structures such as transmission towers, offshore platforms, submerged pipelines and tunnels. With the extensive use of anchors in foundation systems, the understanding of their behaviour has attracted the attentions of researchers for more than half a century (Balla 1961; Sutherland 1965; Meyerhof and Adams 1968; Vesic 1971; Saeedy 1987; Murray and Geddes 1987). Many testing methods have been used to study the behaviour of the anchor, including large-scale field testing, laboratory model testing, and theoretical analyses. Many of these tests and analyses have been performed to understand the failure mode in an earth anchor (Ilamparuthi et al. 2002) and displacement fields (Carr and Hanna 1971).

However, the discrepancies between the prediction and actual behaviour of an anchor are still varying in an extensive range. It is believed that these discrepancies are due to the lack of full understanding of the anchor-soil interaction.

This paper is to examine the displacement field around an uplifting anchor in sand using digital image cross-correlation (DIC). The results from this study show that DIC is a very useful tool in geotechnical research and the displacement and strain fields from this study agree generally the results published by other researchers. This study improves our understanding of the anchor-soil system.

## 2 EXPERIMENTAL SET-UP AND TEST PROCEDURE

### 2.1 Equipment Set-up

An experimental test set-up is developed in this research, which consists of a mono Complementary metal–oxide–semiconductor (CMOS) camera, a test table, a loading frame, a Plexiglas mould, and a PC, as schematically shown in Fig. 1.

The camera is PixeLink PL-B741E model camera with a resolution of 1280 x 1024 pixels from PixeLink (*3030 Conroy Road, Ottawa, ON K1G 6C2 Canada*). A built-in lens in the camera is used to adjust the focus. The camera is set 15 cm away from the model with its optical axis perpendicular to the model. It is controlled by the PC through an in-house developed driver using Matlab® Simulink commands. The frame rate for image capturing is set as 1 frame per second during uplifting.

The loading frame consists of a load cell with a loading capacity of 100 N and a linear displacement transducer (LVDT) with a linear strike of ± 25 mm. The data acquisition system has been developed to acquire the loads and displacements in the anchor during uplifting, which consists of NI-6011E PC card and SCB-68 shielded connector from National Instruments (*11500 N Mopac Expwy, Austin, TX 78759, USA*) and an in-house developed driver in Labview.

The Plexiglas mould has dimensions of 500 mm (length) x 300 mm (width) x 400 mm (depth). A semicircular anchor with a diameter of 50 mm and a thickness of 6 mm is used in this study. A 1 m long threaded steel rod with a diameter of 6 mm is used to connect to the anchor. The anchor is tightened between by two screws attached to the top and bottom of the model anchor. The rod is then connected to the loading frame through an adaptor. The load cell and the LVDT are attached to the rod to measure the load and deformation in the anchor during uplifting, as shown in Fig. 1.

Load was applied vertically through a screw mechanism. The anchor is lifted along a guideslot upward by manually rotating the handle while the images and the load and deformation are acquired simultaneously.

## 2.2 Soil Properties

In order to study the influence of soil density, two conditions are investigated in this research; one is loose and the other is dense. The maximum dry unit weight is tested at 16.95 KN/m3 according to ASTM D-698. The minimum dry unit weight is tested at 13.8 KN/$m^3$ by pouring from a funnel.

The soil conditions with dry unit weights of 14.6 KN/$m^3$ and 16.0 KN/$m^3$ are used in the tests, which represent relative density of 27 % and 71 %. Typical soil properties are shown in Table. 1.

The sand is classified as SP uniformly graded according to Unified Soil Classification System.

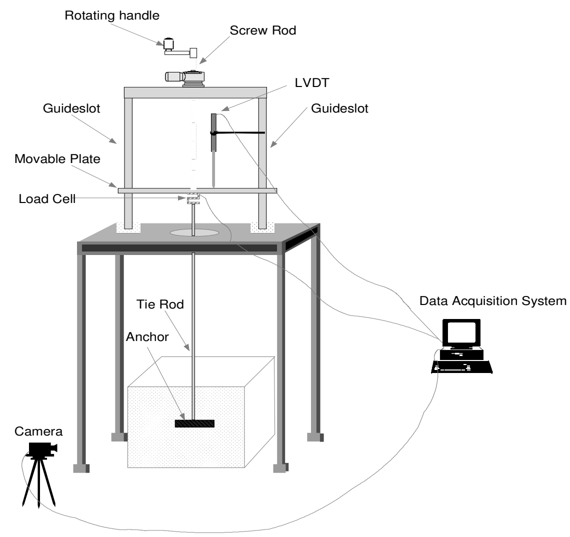


Fig.1 The test set-up for anchor uplifting and image capture

Table 1. Physical and geotechnical properties of sand used in the tests

| State | Uniformity coefficient $C_u$ | Coefficient of curvature $C_c$ | Effective grain size $D_{10}$ (mm) | Specific gravity Gs | Relative density Dr | Angle of friction (degrees) |
|---|---|---|---|---|---|---|
| Loose | 1.29 | 0.98 | 0.56 | 2.65 | 27 | $29^o$ |
| Dense | 1.29 | 0.98 | 0.56 | 2.65 | 71 | $41^o$ |

## 2.3 Sample Preparation

The density of soil samples is controlled by pouring and tamping. As for the loose sample, first, a 50 mm thick sand bed is first placed at the bottom of the mould. Second, the semicircular anchor is set on the sand bed and aligned vertically through the guide slot and horizontally against the front window of the Plexiglas mould. Third, the top sand is prepared by the controlled pluviation method to pour sands from a 5 cm height through a funnel to the required embedment depth of anchor. As for the dense sample, the same steps are followed, but in each step, the sand is compacted by layer by layer by tamping until the final height is reached.

In order to investigate the influence from the embedment depth, three embedment conditions with H/D ratios of 1, 2, and 3 are studied in this research, where H is the anchor embedment depth, D is the anchor diameter.

## 2.4 Test Procedure

First, the data acquisition and image capture drivers are activated in the PC. Second, the camera is first set at 15 cm away with its optical axis perpendicular to the box front window and the image focus and the light intensity are set by adjusting the lens and the aperture. Since the image analysis is very sensitive to the changes in ambient light, the light source for illuminating the sand surface is the only one left on while the rest is off with a dark room during the tests. Third, the camera is set in an auto data acquisition mode with a desired image frame rate, 1 frame per second used in this study. The data acquisition for the load and the displacement are set at a 300 data per second rate. Fourth, the anchor is lifted up by rotating the handle while the images and data are acquired and imported to the computer for the future process. Fifth, the test is terminated until an apparent failure rupture is observed in the sample and no additional loading can be taken by the anchor.

# 3 IMAGE PROCESSING

DIC is used in this study to calculate the displacement field between two consecutive images taken during anchor uplifting. DIC is a classic pattern recognition technique where two images are compared to obtain the relative displacement between them. DIC is widely used in many engineering fields to obtain spatial deformation patterns, albeit with several names, in particular Particle Image Velocimetry (PIV).

The discrete form of standard cross-correlation function is as follows:

$$C(\Delta x,\Delta y)=\frac{1}{MN}\sum_{m=0}^{M-1}\sum_{n=0}^{N-1} f(m,n)\ g(m+\Delta x,n+\Delta y) \qquad [1]$$

Where $M$ and $N$ are the dimensions of the interrogated images, f and g are the intensities of two images being interrogated. The correlation function given above is sensitive to the average intensity of images. Therefore, the zero normalized cross-correlation function is normally used in the analysis.

In this paper, the demo version 3.0 of PIVview2c software is used to calculate the field displacement. This software has features to allow users to select the window size, cross-correlation algorithm, peak function, etc. More details can be found in PIVTEC (2006). Unless noted, the features used in this research are final window size 32 X 32 pixels, the multiple-correlation algorithm, and the multi-grid interrogation method.

# 4 RESULT ANALYSES

## 4.1 Loading Capacity of an Uplift Anchor

The load vs. displacement curves for both loose and dense conditions are shown in Fig. 2. The uplift resistance shows a rapid increase with the displacement at the initial stage up to approximately 2 mm for anchors in both loose and dense conditions. The similar tendency is noticed regardless the embedment depth.

For anchors embedded in loose sand as shown in Fig.2. (a), there are only two phases noted in the tests: the initial phase and the peak phase. The ultimate uplift resistance, although vibrating at a relative mild extent, stays at the peak value until the displacement reaches 15 mm. For dense samples, the third phase is noticed in addition to the two phases in the loose condition, the residual phase. For anchors embedded in dense sand as shown in Fig2. (b), the uplift resistance, after arriving at the peak, showed a gradual decrease with the increasing displacement.

In order to see the influence of the embedment depth on the pullout resistance, a normalized chart is developed along with published data from other researchers, shown in Fig. 3. The breakout factor is defined as

$$Fq = Q_f/\gamma AH \qquad [2]$$

Where $Q_f$ is the ultimate pullout load measured from the tests, H is the anchor embedment depth, γ is the dry unit weight of the sample, and A is the area of the anchor. The results show that the results from this study are consistent with published data by other researchers.

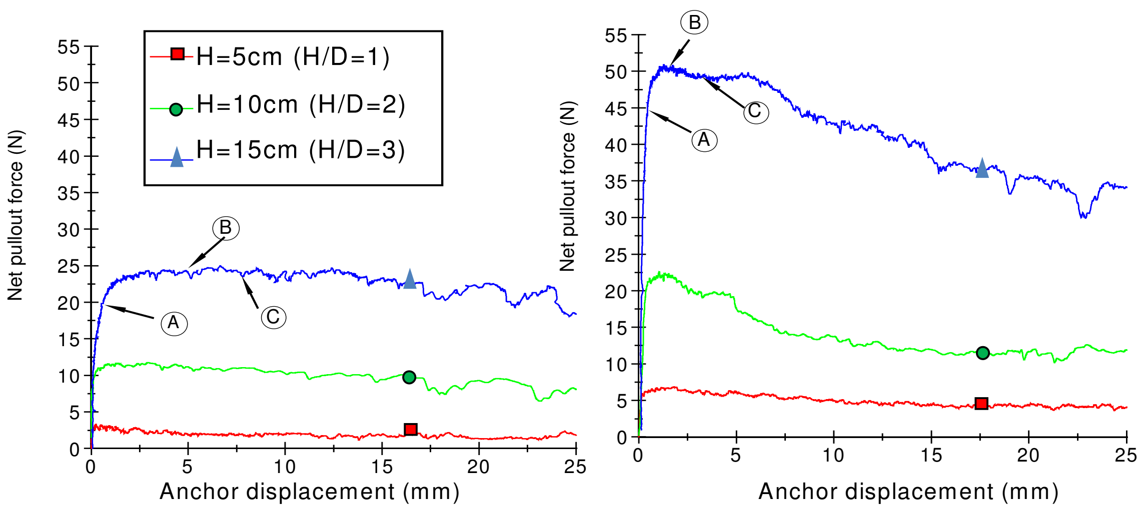


(a) Anchors embedded in loose sand (b) Anchors embedded in dense sand

Fig. 2 The load vs. displacement curves for the anchor

## 4.2 Displacement Field around an Uplifting Anchor

The displacement fields at different phases can be calculated by cross-correlating two images taken at corresponding stages. In this paper, only the displacement fields at the peak phase for 15 cm embedment tests are presented. The label B in Fig. 2 notes the corresponding time where these pair images are taken for the analyses. The displacement fields for both dense and loose conditions at the peak phase are shown in Fig. 4.

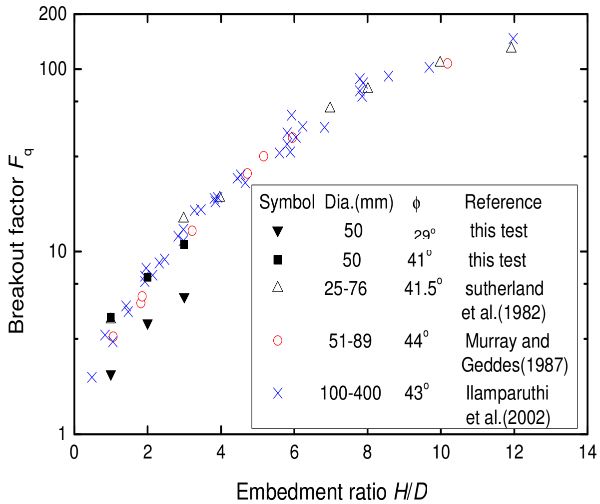


Fig. 3 Breakout factors with published data

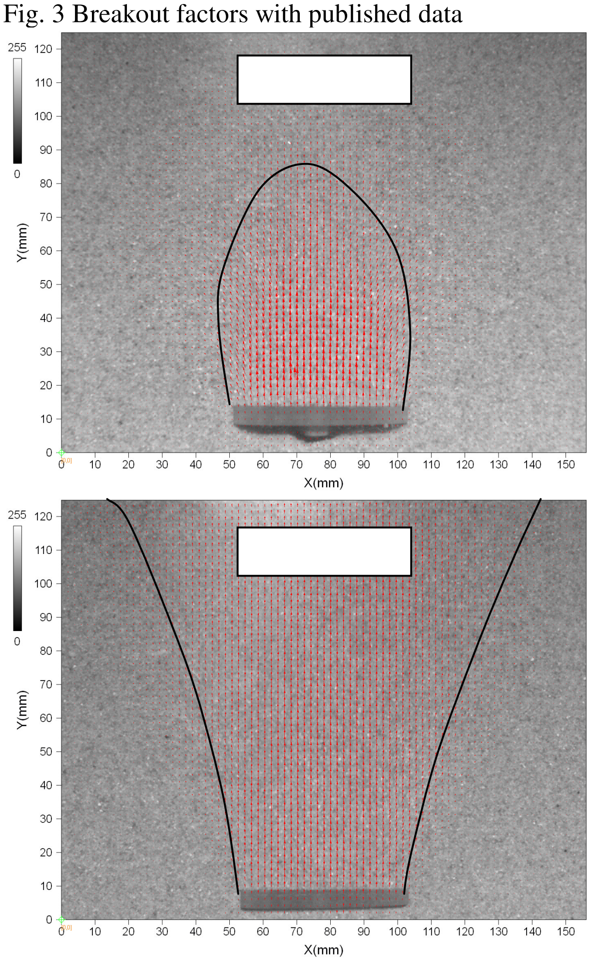


Fig. 4 The displacement fields at peak stage (the embedment depth of 15 mm)

It shows clearly the compaction phenomenon in loose sand conditions, as shown in Fig. 3a. A similar displacement pattern is concentrated within a bell zone above the anchor in loose sand tests. Compared to the loose sand test, a whole block above the anchor has the similar displacement in the area above the anchor in dense sand tests, which extends from the edge of anchor to the sides with an angle of 17$^{o}$ from the vertical.

### 4.3 Strain Field around an Uplifting Anchor

Strains can be calculated using the predicted displacements per Roscoe et al. (1963) and Yamamoto and Kusuda (2001). The displacements for each image window were considered to be the same as the displacements at its centre point. This assumption can be proved to be reasonable if the movement is relatively small. The failure plane can be studied approximately by identifying the maximum shear strains. The contours of shearing strain field for both loose and dense conditions are shown in Fig. 5. The shearing strain filed clearly shows the shearing zone at the right and left edges of anchor plat, though some asymmetrical contours are noticed due to the heterogeneous sample and errors from image processing. In loose sample, the shear bands form a bell-shaped compaction zone. In dense sample the shear bands begin from the upper edge of the anchor plate and extend outward to the ground surface with an inclination angle with the vertical line at approximately 17$^{o}$, which is between 1/3 and ½ ϕ ($\phi$=41$^{o}$ in this study).

## 5 CONCLUSIONS

A displacement field around a scaled semi-circular anchor during uplifting is obtained using digital image cross-correlation (DIC). An optical test set-up is developed in this research to capture the deformation during loading, which consists of a camera, a loading frame, and a PC. Two dry sand samples are used in the investigation: one is in loose condition and the other in dense. A series of images are taken from the camera while the semi-circular anchor is being uplifted against the side-window of a Plexiglas mould. The displacement fields are calculated using DIC and the corresponding strain fields are deduced from the displacement fields. There are distinctive differences between the displacement fields between the loose and dense conditions. In the loose samples a compaction phenomenon is noticed within a bell zone just above the anchor. In dense sample, a whole block with a similar displacement pattern extends from the anchor edge upward with approximately 17$^{o}$ from the vertical. The similar shear bands are also noticed from the strain fields. This study improves the understanding of the failure and loading capacity of an uplift anchor in cohesionless soil.

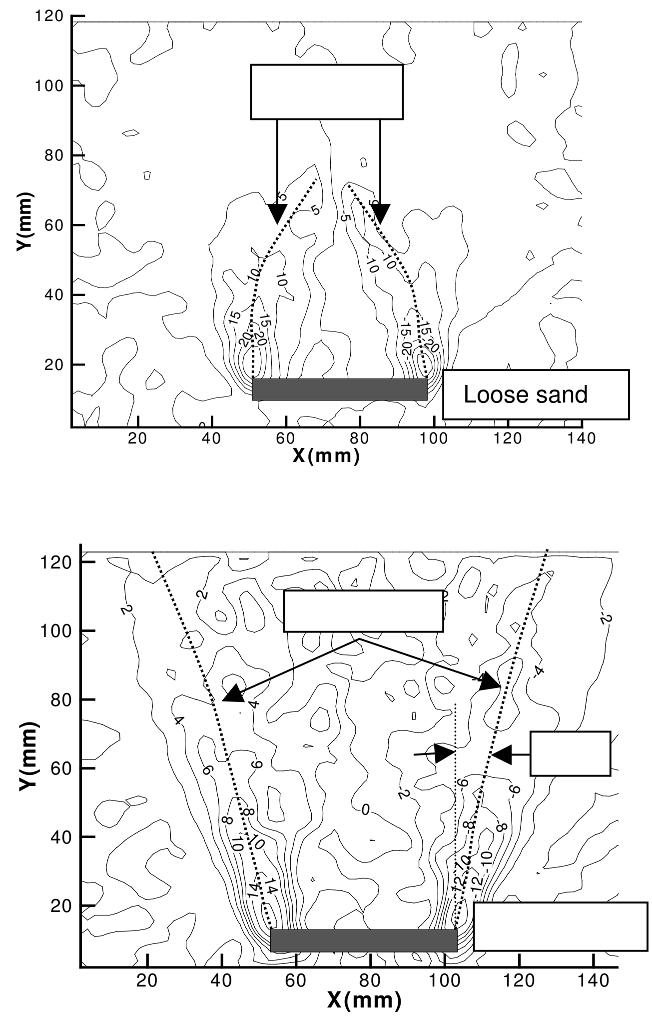


Fig.4. The contours of the shear strain fields

6 ACKNOWLEDGEMENTS

The authors acknowledge the financial support of the Seed Fund awarded to the first author. The authors also want to thank the China Scholarship Council for the scholarship awarded to the second author during his one-year study at Ryerson University.

References

Balla, A. (1961). "The resistance to breaking out of mushroom foundations for pylons." *Proc. of the 5th ICSMFE*, Paris, 569-576.

Carr, R.W. and Hanna, T. H. (1971). "Sand movement measurements near anchor plates." *J. of the Soil Mech. and Found. Div., ASCE*, 97, 833-840.

Hanna, T. H., Sparks, R., and Yilmaz, M. (1972). "Anchor behavior in sand." *American Society of Civil Engineers, Journal of the Soil Mechanics and Foundations Division*, 98(SM11), 1187-120.

Ilamparuthi, K., Dickin, E. A., and Muthukrisnaiah, K. (2002). "Experimental investigation of the uplift behaviour of circular plate anchors embedded in sand." *CGJ*, 39(3), 648-664.

Meyerhof, G. G., and Adams, J. I. (1968). "The ultimate uplift capacity of foundations." *CGJ*, 5, 225-244.

Murray, E. J., and Geddes, J. D. (1987). "Uplift of anchor plates in sand." *J. of Geot. Eng., ASCE*, 113(3), 202-215.

PIVTEC GMBH (2006). *PIVview User Manual*Ver.2.4, http://www.pivtec.com/.

Roscoe, K., Arthur, J., and James, R. 1963. "The determination of strains in soils by an X-ray method". *Civil Engineering and Public Works Review*, 58: 873-876 and 1009-1012.

Saeedy, H. S. (1987). "Stability of circular vertical anchors." *CGJ*, 24(3), 452-456.

Sutherland, H. B. (1965). "Model studies of shaft raising through cohesionless soils." *Proc.of the 6th ICSMFE,* Montreal, 410-413.

Sutherland, H. B. (1988). "Uplift resistance of soils." *Geotechnique*, 38(4), 493-516.

Vesic, A. S. (1971). "Breakout resistance of objects embedded in ocean bottom." *ASCE, J. of the Soil Mech. and Found. Div.*, 97(9), 1183-1203.

Yamamoto, K. and Kusuda, K. (2001). "Failure mechanism and bearing capacities of reinforced foundations." *Geotextiles and Geomembranes*, 19(3): 127-162.